ARTICLE

Oxidative Coupling of Methane over Li/MgO: Catalyst and Nanocatalyst Performance

Ali Farsi[a,b*], Ali Moradi[a], Sattar Ghader[a], Vahid Shadravan[a,b]

a. Department of Chemical Engineering, Shahid Bahonar University of Kerman, Kerman, Iran
b. Young Researchers Society, Shahid Bahonar University of Kerman, P. O. Box 76175-133, Iran

(Dated: September 27, 2010; Accepted on December 9, 2010)

The Li/MgO catalyst and nanocatalyst were prepared by the incipient wetness impregnation and sol-gel method, respectively. The catalytic performance of the Li/MgO catalyst and nanocatalyst on oxidative coupling of methane was compared. The catalysts prepared in two ways were characterized by X-ray powder diffraction, Brunauer-Emmett-Teller surface and transmission electron microscope. The catalyst was tested at temperature of 973–1073 K with constant total pressure of 101 kPa. Experimental results showed that Li/MgO nanocatalyst in the oxidative coupling of methane would result in higher conversion of methane, higher selectivity, and higher yield of main products (ethane and ethylene) compared to ordinary catalyst. The results show the improved influence of nanoscale Li/MgO catalyst performance on oxidative coupling of methane.

Key words: Oxidative coupling of methane, Nanocatalyst, Sol-gel

I. INTRODUCTION

The oxidative coupling of methane (OCM) ($2CH_4+O_2 \rightarrow C_2H_4+2H_2O$, $\Delta G^{\ominus}_{1000\ K}$=–159.7 kJ/mol) is an attractive reaction which can be used for more effective usage of natural gas because considerable amount of methane exists in natural gas [1–3]. OCM reaction is thermodynamically more favorable compared to direct coupling reaction of methane without an oxidant ($2CH_4 \rightarrow C_2H_6+H_2$, $\Delta G^{\ominus}_{1000\ K}$=71 kJ/mol) [4]. The OCM reaction is extensively studied [5–9]. However, no catalysts could reach the principal criteria for industrial application of OCM [10, 11]. OCM reaction has more selectivity to CO_x (CO and CO_2) production than C_{2+} (ethylene and ethane) products and the one pass yield of total C_{2+} was lower than the economic threshold [12].

The challenges that limit the commercialization of OCM process are: (i) high temperature (973–1173 K) to achieve high C_{2+} yield, (ii) the active sites in the coupling catalysts also activate the C–H bond in C_{2+}, resulting in the formation of CO_2 by combustion, (iii) limitation on methane conversion (<45%) and C_{2+} yield (<27%) imposed by the explosion limit of oxygen concentrations in the feed, (iv) low concentrations of ethylene in the product, making the separation of the product stream uneconomical, (v) low selectivity at higher conversion, making the achievement of simultaneous good selectivity and conversion extremely difficult, (vi) short lifetime for catalysts containing volatile promoters [10, 13, 14].

Some of these problems can be overcome by use of nanocatalyst. An important feature of nanocatalyst is that its surface properties can be very different from ordinary catalysts. Although the size of nanoparticles cannot be exactly controlled during synthesis, it is possible to narrow the size distribution by controlling the reaction conditions. Complete control over the size distribution requires size selection techniques. In this way, the activity and selectivity of nanocatalysts are strongly dependent on their size, shape, and surface structure, as well as their composition. Recently, nanocatalysts have attracted much attraction [15–19]. In comparison with their micro-sized counterparts, nanocatalysts show higher activity, better selectivity, and outstanding stability because of their large specific surface area, high percentage of surface atoms and special crystal structures. Nanoparticles can be synthesized by several methods such as sol-gel processing, micro-emulsion, homogeneous precipitation, gas evaporation, laser vaporization, ionized beam deposition, freeze drying and *etc.* [16, 18, 20].

Alkali promoted MgO catalyst with no formal redox properties is a promising catalyst for OCM [21]. One of the best catalysts is Li/MgO with or without promotion [21–27]. Ito *et al.* suggested that for these catalysts [Li^+O^-] type defect sites are responsible for the catalytic activity [26]. Further, it was suggested that hydrocarbon activation occurs on these sites forming alkyl radicals, followed by reactions in the gas phase to form products. Also, Myrach *et al.* investigated

*Author to whom correspondence should be addressed. E-mail: ali.farsi@gmail.com, Tel.: +98-913-3875507

the role of Li in the MgO matrix and studied the catalyst morphological, optical, and magnetic properties as a function of Li for OCM reaction [27]. They elucidated two model systems which described the place of Li on MgO films. Their results showed that at 700 K, Li starts segregating towards the surface and forms irregular Li-rich oxide patches and at 1050 K, Li desorbs from the MgO surface, leaving behind a characteristic defect pattern. Their results not only explain the driving forces for Li segregation towards the MgO surface, but also rationalize the absence of $[Li^+O^-]$ centers. The works on the Li/MgO catalysts have focused on the use of different preparation methods for Li/MgO catalyst synthesis with changing Li percentage in the catalyst [26, 28] or adding some transition metal to Li/MgO to understand its effect on methane conversion and products yield [22–24], while the catalyst shape, size, active sites, oxides surface and morphology have also influence on catalytic properties of Li/MgO catalyst [27, 29, 30]. However, less works have been performed on the second subject and many questions should be addressed especially the effect of using nanocatalyst on OCM reaction.

In this work, an nanosized Li/MgO catalyst prepared by sol-gel method is used for the OCM. It is shown that the nanocatalyst is more active and selective to C_{2+} products, than an equivalent catalyst prepared by conventional impregnation method (referred to as ordinary catalyst). Nanocatalyst activity in terms of methane conversion, C_{2+} selectivity, and yield are compared to ordinary catalysts and some improvements are observed.

II. EXPERIMENTS

A. Catalyst preparation

The 7% Li/MgO catalysts for OCM reaction were prepared by the incipient wetness impregnation and sol-gel method. All chemicals involved during preparation of catalysts including $Mg(OCH_3)_2$ (with the purity of 99%) and $LiNO_3$ (99%) were purchased from Aldrich. A programmable tubular furnace (Heraeus model RO 4/50) was used for calcinations of catalyst.

1. Li/MgO catalyst

The Mg $(OCH_3)_2$ powders were impregnated with the aqueous solutions of $LiNO_3$ in appropriate concentration at 60 °C. This solution was evaporated at 100 °C to dryness for 20 min, and then dried overnight at room temperature. Finally, the resultant was calcined in air for 4 h at 850 °C.

2. Li/MgO nanocatalyst

A solution of $Mg(OCH_3)_2$ in methanol and $LiNO_3$ were added to a vessel with a desired ratio, which was stirred vigorously for 20 min before the addition of appropriate amounts of water, and with vigorously stirring to complete the gelation at 60 °C (wet gel). The dryness was carried out at 100°C in vacuum for 3 h, then the dried gels were calcined at 850°C in air for 4 h.

B. Catalyst characterization

The phase structure of the catalyst and nanocatalyst were characterized by powder X-ray diffraction (XRD). It was obtained in ambient air in the 2θ range of 10°–80° on a Rigaku diffractometer (RINT 1200) using Cu Kα radiation operated at 40 kV and 20 mA. Samples were mounted on a Pt plate with a thermocouple and heated at 0.167 K/s in air. The intensity was measured during 5–10 s. The average crystallite size (ACS) was estimated by the broadened peak width using the Scherrer formula (Eq.(1))[28].

$$\mathrm{ACS} = \frac{0.94\lambda}{B\cos\theta} \tag{1}$$

here λ is the wavelength, and B is the calibrated half-peak width of the XRD lines at the Bragg diffraction angle θ.

Brunauer-Emmett-Teller (BET) surface area was measured with a Belsorp 28SA (Japan Bell Ltd) at 77 K using N_2. For those samples with small surface areas, Kr was used at 77 K and 86.45 kPa. Samples were evacuated at 450 °C for 1 h prior to measurement.

Transmission electron microscope (TEM) images and the particle size were obtained using a Philips CM200 microscope operating at 200 kV. For TEM images, the sample powder was dispersed in methanol by using ultrasonic radiation for 10 min and a drop of the suspension was placed onto the carbon-coated grids.

C. Catalytic activity test

The OCM reaction was carried out using a fixed-bed flow reactor (diameter of 8 mm and length of 0.25 m) with an on-line gas chromatograph. 0.3 g of ordinary catalyst or nanocatalyst was loaded in a micro-reactor in each run at various temperatures (973–1073 K) and total pressure of 101.3 kPa. A K-type thermocouple was appended to the outside wall of the reactor to monitor the furnace temperature. The temperature along the catalyst bed (inside the reactor) was measured by another thermocouple and was monitored by a temperature controller. The flow rates of inlet gases, CH_4 (99.999%), O_2 (99.995%), and N_2 (99.999%) were also controlled by a digital mass flow controller (Brooks 5850), which was calibrated by a 10 mL bubble flow meter. The mixed stream of methane, oxygen, and nitrogen with a flow rate of 150 mL/min was feeded to the reactor. A cold trap was placed at the outlet of the reactor to separate any condensed water from the

DOI:10.1088/1674-0068/24/01/70-76

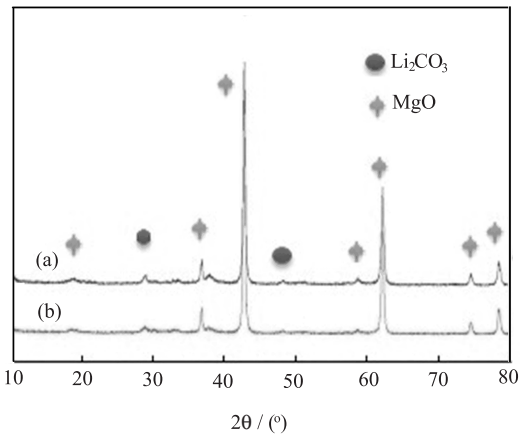

FIG. 1 XRD patterns of Li/MgO (a) ordinary catalyst and (b) nanocatalyst.

reaction products. The exit gas of cold trap was analyzed with an on-line gas chromatograph (GC, model Chrompack 9000) equipped with a Propack-Q packed column, thermal conductivity, and flame ionization detectors.

D. Reaction parameters calculation

The conversion of reactants, the selectivity and the yield of main products were calculated by:

$$X_{\mathrm{CH_4}} = \frac{F_{\mathrm{CH_4,in}} - F_{\mathrm{CH_4,out}}}{F_{\mathrm{CH_4,in}}} \quad (2)$$

$$S_{\mathrm{C_{2+}}} = \frac{2F_{\mathrm{C_{2+},out}}}{F_{\mathrm{CH_4,in}} - F_{\mathrm{CH_4,out}}} \quad (3)$$

$$Y_{\mathrm{C_{2+}}} = S_{\mathrm{C_{2+}}} X_{\mathrm{CH_4}} \quad (4)$$

in which $X_{\mathrm{CH_4}}$ is the conversion of $\mathrm{CH_4}$, $S_{C_{2+}}$ is the selectivity of $\mathrm{C_{2+}}$, $Y_{\mathrm{C_{2+}}}$ is the yield of C_{2+}, F_i is the molar flow rate of component i.

III. RESULTS AND DISCUSSION

A. X-ray diffraction

In order to obtain information about the principal components of ordinary catalyst and nanocatalyst, powder XRD was used to identify phase composition and crystal size in the two catalysts. Figure 1 shows the powder XRD reflections of phases formed in the Li/MgO ordinary catalyst and nanocatalyst. The powder XRD patterns of these two kinds of catalysts were approximately the same, but the peaks corresponding to MgO phase became narrower for Li/MgO ordinary catalyst. In both cases, peaks of Li_2CO_3 could be observed. No other phases of Li, including $LiNO_3$ were detected, indicating that the $LiNO_3$ decomposed completely.

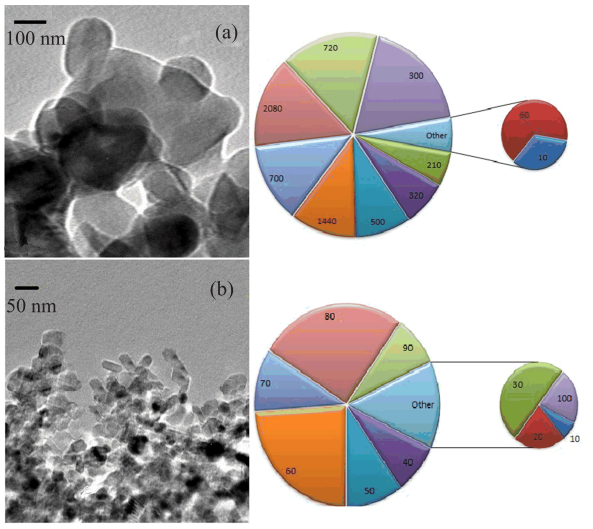

FIG. 2 TEM images and particles size distributions of Li/MgO (a) ordinary catalyst and (b) nanocatalyst.

B. Transmission electronic microscopy

Figure 2 presents the TEM image of Li/MgO nanocatalyst prepared by the sol-gel method and incipient wetness impregnation ordinary catalyst. Figure 2 shows that Li/MgO nanocatalyst had polyhedral morphology and good mono-disparity. The average size of Li/MgO nanocatalyst was 63.4 nm, while the average size of the Li/MgO ordinary catalyst was 566 nm. Figure 2 also gives the difference between particle sizes distributions for two kinds of catalysts. The particle size distribution for nanocatalyst is narrow, in the range of 60–80 nm, but the particle size of Li/MgO ordinary catalyst has a wide range of 500–800 nm. The average particle sizes calculated by powder XRD pattern and Scherrer formula are 71 and 800 nm for nanocatalyst and ordinary catalyst, respectively, which indeed gives more accurate size for nanocatalyst.

C. BET surface

Table I shows the difference BET surface areas of various catalysts prepared by incipient wetness impregnation, sol-gel method, and other different methods [22–27]. Compared to these ordinary catalysts, the nanocatalyst prepared by sol-gel method shows remarkably higher surface area. The surface area of nanocatalyst is 60 m^2/g while relevant surface area for ordinary catalyst is 4.6 m^2/g. The surface area has an influence on the catalyst performance which will be discussed in the subsequent sections.

DOI:10.1088/1674-0068/24/01/70-76

TABLE I Oxidative coupling of methane over various Li/MgO catalysts prepared by different method. The parameters include calcination temperature T_c, reactor temperature T_R, selectivity S_i, conversion X_i, yield Y_i, and weight of catalyst W_c.

Components	Li%	T_c/K	W_c/g	T_R/K	BET/(m^2/g)	CH_4:O_2:inert	X_{CH_4}%	X_{O_2}%	$S_{C_{2+}}$%	$Y_{C_{2+}}$%
$Mg(NO_3)_2$+$LiNO_3$ [40]	5	1073	0.2	1073	2.9	4:1:3.5	19.1	80.5	55.5	10.6
$Mg(OH)_2$+Li[a] [22]	3		0.375	1073	1.2					13.5
Lithium chloride+MgO[b] [23]	14	873	0.55	1023		4.3:1	22.5	42.2	63.4	14.26
Li/MgO[c] [24]	5.3	1123	0.1	1073	2	4.75:1	23		54	12.4
$Mg(OH)_2$+LiOH[c] [25]	1.3	1123	0.375	1073		9.6:1:3.7	20		80	16
Li/MgO[c] [41]	10	1123	0.744	1073	1		12.9	100	75	9.7
Metal nitrate[c] [29]	5	1123		1073		3:1:27.2	33.86		57	19.3
Mg acetate+Li acetate[c] [30]	10	1053	0.5	1023	5		28.9	99.7	66.2	19.13
MgO+Li_2CO_3[c] [42]	1	1073	1.5	1023			37.4	99.1	44.3	17
$Mg(OCH_3)_2$+$LiNO_3$[c]	7	1123	0.3	1073	4.6	3:1:3	26.1	98.7	61.3	16
$Mg(OCH_3)_2$+$LiNO_3$[d]	7	1123	0.3	1073	60	3:1:3	39.6	99.9	66.4	26.3

[a] Wet mixing method.
[b] Mixing of aqueous salt with aqueous suspensions.
[c] Wet impregnation.
[d] Sol-gel.

D. Catalytic performance of Li/MgO ordinary and nanocatalyst

The normally accepted scheme for OCM is as follow [28, 31, 32]. The principal reactions are:

$$2CH_4 + \frac{1}{2}O_2 \rightarrow C_2H_6 + H_2O \quad (5)$$

$$C_2H_6 + \frac{1}{2}O_2 \rightarrow C_2H_4 + H_2O \quad (6)$$

And the main unwanted reactions are:

$$CH_4 + 2O_2 \rightarrow CO_2 + 2H_2O \quad (7)$$

$$CH_4 + \frac{3}{2}O_2 \rightarrow CO + 2H_2O \quad (8)$$

Due to above scheme, methane is first partially oxidized to ethane in reaction (5). A secondary reaction of oxy-dehydrogenation of ethane then proceeds to form ethylene in reaction (6). Two further steps are the non-selective oxidation of methane to carbon dioxide and carbon monoxide (reactions (7) and (8)).

The results of methane conversions in OCM reaction over Li/MgO ordinary and nanocatalyst in different range of temperature and CH_4/O_2 are illustrated in Fig.3(a) and Fig.3(b), respectively. The conversion of methane by the Li/MgO nanocatalyst was apparently higher than ordinary catalyst especially at higher temperatures. To find a sensible reason for this matter, mechanism of Li/MgO on ordinary and nanocatalyst specific surface area and active sites should be investigated.

The nature of methane interaction and catalyst has also effect on the formation of methyl radicals on Li/MgO. Therefore, under high temperature conditions necessary to activate the strong primary C−H bonds in the reactants, much more methane is consumed and conversion increases.

Bytyn *et al.* [33], Mirodatos *et al.* [34], and Lapszewicz *et al.* [35] suggested that first step of methane interaction with the catalyst surface is its dissociative adsorption. Ji *et al.* proposed that combination of tetrahedral and octahedral metallic cores with different oxidation states is responsible for initiating catalytic action in OCM [36]. As a result, it can be concluded that surface of catalyst and its morphology have great and influencing effect on the methane conversion. Therefore, the results obtained in this work can be confirmed because synthesis of catalyst on the nanosize scale provides more specific surface area and greater numbers of active sites for the reaction. It is also demonstrated by TEM image and powder XRD pattern that the active site is more in the nanocatalyst, so reducing metal size, gives better performance for catalyst conversion. In summary, conversion of the sol-gel nanocatalyst is superior to that of Li/MgO ordinary catalyst. This is due to two effects: (i) the sol-gel derived nanocatalyst has a significant higher surface area (60 *vs.* 4.6 m^2/g) and (ii) the sol-gel derived nanocatalyst contains a higher amount of Li incorporated in the MgO matrix. Both effects contribute to an increase in the number of active sites.

Figure 4 shows the results of C_{2+} selectivity in OCM reaction over Li/MgO ordinary and nanocatalyst. Although C_{2+} selectivity increases with temperature in both cases, sol-gel derived Li/MgO is always more selective than the ordinary catalyst. The difference between selectivity is less in high temperatures.

It is expected that surface of a catalyst has great in-

DOI:10.1088/1674-0068/24/01/70-76

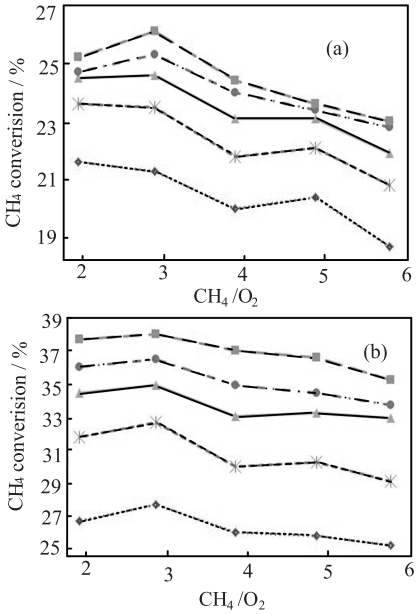

FIG. 3 Profile of methane conversion versus CH_4/O_2 over Li/MgO at different feed temperatures of 1073, 1048, 1023, 998, and 973 K from up to down. (a) Ordinary catalyst and (b) nanocatalyst.

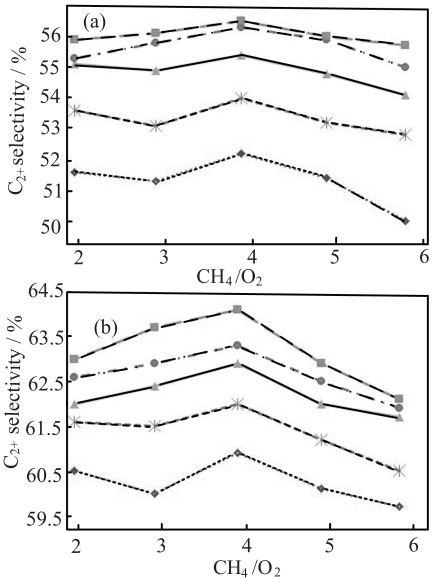

FIG. 4 Profile of C_{2+} selectivity versus CH_4/O_2 over Li/MgO catalyst at different feed temperatures of 1073, 1048, 1023, 998, and 973 K from up to down. (a) Ordinary catalyst, (b) nanocatalyst.

fluence on its properties. In this work a nanocatalyst is employed, whose structural properties is tuned to some extent and a nanosized catalyst is obtained. The correlation between catalyst structure and reactivity should help to elucidate the reaction mechanisms and provide important insights into structural factors governing reaction kinetics and results observed.

According to the report of Ito *et al.* [26], in the OCM reaction methane and oxygen react in a way that O^- of Li/MgO catalyst will react with methane on the catalyst surface and as a result, if more O^- would be available for reaction, more reaction in the desired way is expected. The amount of O^- on surface would be more in the case of nanocatalyst. However, some of OCM reactions proceed in gas phase which result in CO_x. Nevertheless, it is the role of Li/MgO that leads to the desirable products because these reactions proceed on surface of catalyst. With nanocatalyst the surface and active area is increased and rate of surface reactions become more important compared to gas phase reaction. As a result desirable products (C_{2+}) become more and selectivity in the case of nanocatalyst would be more.

The difference in C_{2+} selectivity of two catalysts was more at low temperatures while it became less at higher temperatures. The reactivity of a catalyst often depends very sensitively on microscopic structure of the catalyst, *e.g.* on particle size and morphology, the presence of specific active centers or an active metal-support interface and the role of surface species during the reaction is of great importance. Therefore, high difference between C_{2+} selectivity of Li/MgO nanocatalyst and Li/MgO ordinary catalyst at low temperatures can be explained by events which occur for both ordinary and nanocatalyst structures. It is widely accepted that the addition of alkali ions (Li, Na, K) into the metal oxide like Li/MgO causes the inhibition of total oxidation of methane, resulting in ethane and ethylene selectivity enhancement [36–38]. It has also been realized that high basicity of a catalyst is necessary to enhance the C_{2+} selectivity in OCM reaction. The addition of Li into MgO increases the basicity of the catalyst, hence producing good OCM activity. This is the major reason for the large use of alkali metal compounds additives, because they result in loss of surface area caused by sintering. It was also noted that in oxidation catalyst, too large surface area favors consecutive reactions, leading to deep oxidation. Therefore, during the OCM reaction over the nanocatalyst low temperatures favors the interaction between carrier and active component to form more active sites and also new sites is formed. However, overheating can result in the surface sintering and the reduction of specific surface area, which in turn leads to the reduction in catalytic selectivity. At higher temperature (above 1000 K) selectivity of nanocatalyst becomes less compared to ordinary catalyst. Above the 800 °C some of Li desorbs from the MgO surface, leaving behind a decrease in selectivity [27]. However, one may expect most of the Li ions to be expelled from the solid-solid solution taking into account both the high calcination temperature applied (850 °C) and the high Li content (7%). Furthermore, undesired reactions become more important at high temperatures and as a result the difference between selectivities of nanocata-

DOI:10.1088/1674-0068/24/01/70-76

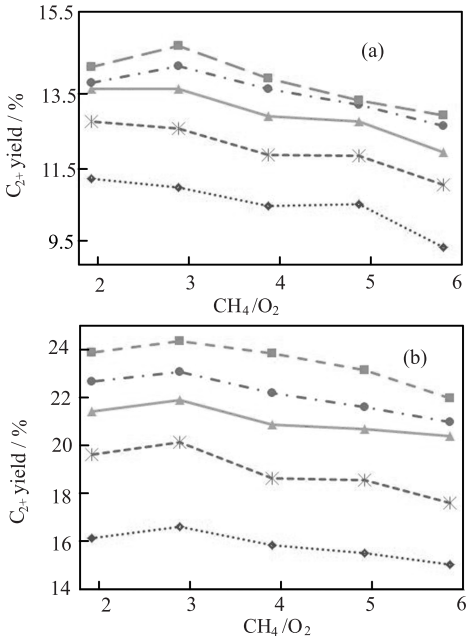

FIG. 5 Profile of percent of C_{2+} yield versus CH_4/O_2 over Li/ MgO at different feed temperatures of 1073, 1048, 1023, 998, and 973 K from up to down. (a) Ordinary catalyst, (b) nanocatalyst.

lyst and ordinary catalyst becomes less.

The yield data clearly illustrate the advantage of Li/MgO nanocatalyst (Fig.5(b)) compared to Li/MgO ordinary catalyst (Fig.5(a)). In summary, the two catalysts show quite different activity which can be explained by characterization results and related literature [22–27, 29, 30, 36–42]. Complex reactions occur at the catalyst surface and in the surrounding gas phase, and the reactions on the surface will have a positive effect on the product yield.

The nanocatalyst performance results including methane conversion, C_{2+} selectivity, and yield are compared to relevant nine works on Li/MgO catalysts [22–25, 29, 30, 40–42] and reported in Table I. These previous studies [22–25, 29, 30, 40–42] show that the prevailing factor that influences C_{2+} yield is BET surface area compared to amount of Li in the ordinary catalysts. As a result, it is not surprising that one of the most of C_{2+} yield is available because their ordinary catalyst has the most surface area. Compared to these works the BET of Li/MgO nanocatalyst is more and we expect more yield as extent of surface reactions is increased compared to gas phase reactions.

As shown in Table I, for the OCM reaction with Li/MgO, the highest CH_4 conversion (38%) was obtained by Skutil *et al.* [42] when temperature was 1023 K and CH_4/O_2=2, whereas the highest C_{2+} selectivity (80%) was attained by McNamara *et al.* at temperature of 1073 K and CH_4/O_2=9.6 [25]. Skutil *et al* obtained high conversion because they used low methane to oxygen ratio [42]. Hence, methane conversion is likely to take place together with methane combustion. This is the reason why their respective C_{2+} selectivity is not as high as the one obtained by McNamara *et al.* [25]. In contrast, the Li concentration used by both Skutil *et al.* [42] and McNamara *et al.* [25] is different, therefore producing different OCM activity. However, McNamara *et al.* reported that the basicity and low surface area of the catalyst is the reason for obtaining such results [25]. Table I shows the most important result that the surface area of catalyst has a prevailing influence on the catalyst activity, and therefore it is reasonable to observe better activity in the case of nanocatalyst as conversion is more in the case of nanocatalyst.

IV. CONCLUSION

The 7%Li/MgO catalysts for OCM reaction were prepared by the sol-gel and incipient wetness impregnation method. The sol-gel method was used to make Li/MgO nanocatalyst while ordinary standard catalyst was obtained by impregnation method. The dryness and calcinations of both ordinary and nanocatalyst were at the same temperature. The catalytic performance of the nanocatalysts on OCM was investigated and compared with that of ordinary catalyst. The conversion of methane, C_{2+} selectivity, and main products yield of Li/MgO nanocatalyst were higher compared to those of the ordinary catalyst. Compared to other nine previous work with other Li/MgO ordinary catalysts which are given in the literature, the effect of nanocatalyst on catalyst activity is elucidated to some extent.

V. ACKNOWLEDGMENTS

The authors would like to highly appreciate Prof. Dr. Ir. Leon Lefferts from University of Twente and Prof. Zainuddin Abdul Manan from University of Teknologi Malaysia for their valued comments, suggestions as well as their critical discussions throughout this research.

[1] J. Santamaría, M. Menéndez, J. A. Peña, and J. I. Barahona, Catal. Today **13**, 353 (1992).
[2] W. Kiatkittipong, T. Tagawa, S. Goto, S. Assabumrungrat, K. Silpasup, and P. Praserthdam, Chem. Eng. J. **115**, 63 (2005).
[3] J. Williams, R. H. Jones, J. M. Thomas, and J. Kent, Catal. Lett. **3**, 247 (1989).
[4] S. Liu, X. Tan, K. Li, and R. Hughes, Catal. Rev. **43**, 147 (2001).
[5] G. E. Keller and M. M. Bhasin, J. Catal. **73**, 9 (1982).
[6] S. Sugiyama and J. B. Moffat, Energy Fuels **8**, 463 (1994).
[7] Z. Stansch, L. Mleczko, and M. Baerns, Ind. Eng. Chem. Res. **36**, 2568 (1997).

DOI:10.1088/1674-0068/24/01/70-76

[8] H. Zhang, J. Wu, B. Xu, and C. Hu, Catal. Lett. **106**, 161 (2006).
[9] J. Miao, G. Song, Y. Fan, and J. Zhou, Chin. J. Catal. **29**, 1277 (2008).
[10] M. Y. Sinev, Z. T. Fattakhova, V. I. Lomonosov, and Y. A. Gordienko, J. Nat. Gas Chem. **18**, 273 (2009).
[11] V. R. Choudhary and B. S. Uphade, Catal. Surv. Asia **8**, 15 (2004).
[12] A. Machocki and R. Jezior, Chem. Eng. J. **137**, 643 (2008).
[13] R. Spinicci, P. Marini, S. De Rossi, M. Faticanti, and P. Porta, J. Mol. Catal. A **176**, 253 (2001).
[14] T. V. Choudhary and D. W. Goodman, Catal. Today **77**, 65 (2002).
[15] Q. Shu, B. Yang, H. Yuan, S. Qing and G. Zhu, Catal. Commun. **8**, 2159 (2007).
[16] J. D. Aiken and R. G. Finke, J. Mol. Catal. A **145**, 1 (1999).
[17] T. R. Thurston and J. P. Wilcoxon, J. Phys. Chem. B **103**, 11 (1999).
[18] Y. He, B. Yang, G. Cheng, and H. Pan, Powder Technol. **134**, 52 (2003).
[19] S. W. Guo, L. Konopny, and R. Popovitz-Biro, Adv. Mater. 12, 302 (2000).
[20] Y. He, B. Yang, and G. Cheng, Catal. Today **98**, 595 (2004).
[21] J. M. DeBoy and R. F. Hicks, Ind. Eng. Chem. Res. **27**, 1577 (1988).
[22] H. M. Swaan, Y. Li, K. Seshan, J. G. Van Ommen, and J. R. H. Ross, Catal. Today **16**, 537 (1993).
[23] E. V. Shischak, M. S. Kazi, I. P. Dzikh, S. S. Abadjev, and V. U. Shevchuk, React. Kinet. Catal. Lett. **61**, 83 (1997).
[24] J. A. Roos, A. G. Bakker, H. Bosch, J. G. V. Ommen, and J. R. H. Ross, Catal. Today **1**, 133 (1987).
[25] D. J. McNamara, S. J. Korf, K. Seshan, J. G. V. Ommen, and J. R. H. Ross, Can. J. Chem. Eng. **69**, 883 (1991).
[26] T. Ito, J. X. Wang, C. H. Lin, and J. H. Lunsford, J. Am. Chem. Soc. **107**, 5062 (1985).
[27] P. Myrach, N. Nilius, S. V. Levchenko, A. Gonchar, T. Risse, K. P. Dinse, L. A. Boatner, W. Frandsen, R. Horn, H. J. Freund, R. Schlögl, and M. Scheffler, ChemCatChem **7**, 854, (2010).
[28] W. Y. Tung and L. L. Lobban, Ind. Eng. Chem. Res. **31**, 1621 (1992).
[29] L. Olivier, S. Haag, H. Pennemann, C. Hofmann, C. Mirodatos, and A. C. V. Veen, Catal. Today **137**, 80 (2008).
[30] V. R. Choudhary, S. A. R. Mulla, and B. Uphade, J. Chem. Technol. Biotechnol. **72**, 99 (1998).
[31] L. Lehmann and M. Berns, J. Catal. **135**, 467 (1992).
[32] A. Farsi, A. Moradi, S. Ghader, V. Shadravan, and Z. A. Manan, J. Nat. Gas Sci. Eng. **5**, 270 (2010).
[33] W. Bytyn and M. Baerns, Appl. Catal. **28**, 199 (1986).
[34] C. Mirodatos and G. A. Martin, Fuel Process Technol. **42**, 179 (1995).
[35] A. Lapszewicz and X. Z. Jiang, Catal. Lett. **13**, 103 (1992).
[36] S. Ji, T. Xiao, S. Li, C. Xu, R. Hou, K. S. Coleman, and M. L. H. Green, Appl. Catal. A **225**, 271 (2002).
[37] K. Murata, T. Hayakawa, S. Hamakawa, and K. Suzuki, Catal. Today **45**, 41 (1998).
[38] S. Takaneka, T. Kabarugi, I. Yamanaka, and K. Otsuka, Catal. Today **71**, 31 (2001).
[39] L. S. Birks and H. Friedman, J. Appl. Phys. **17**, 687 (1946).
[40] J. S. Ahari, R. Ahmadi, H. Mikami, K. Inazu, S. Zarrinpashne, S. Suzuki, and K. I. Aika, Catal. Today **145**, 45 (2009).
[41] S. J. Korf, J. A. Roos, J. M. Diphoorn, R. H. J. Veehof, J. G. V. Ommen, and J. R. H. Ross, Catal. Today **4**, 279 (1989).
[42] K. Skutil and M. Taniewski, Fuel Process Technol. **88**, 877 (2007).

DOI:10.1088/1674-0068/24/01/70-76